# Dielectric properties of poly- and single-crystalline Ba1-xSrxTi205

*Materials Transactions*, Vol. 48, No. 5 (2007) pp. 984 to 989


# Dielectric Properties of Poly- and Single-Crystalline $Ba_{1-x}Sr_xTi_2O_5$

XinYan Yue, Rong Tu and Takashi Goto

*Institute for Materials Research, Tohoku University, Sendai 980-8577, Japan*

Poly- and single-crystalline SrO substituted $BaTi_2O_5$ ($Ba_{1-x}Sr_xTi_2O_5$) were prepared by arc-melting and floating-zone (FZ) melting, respectively. Both showed a strong *b*-axis orientation and had maximum permittivity ($\varepsilon_{max}$) at 1 mol% SrO substitution. The $\varepsilon_{max}$ values of poly- and single-crystalline $Ba_{0.99}Sr_{0.01}Ti_2O_5$ were 3300 and 42190, respectively. The Curie temperatures ($T_c$) of poly- and single-crystalline $Ba_{1-x}Sr_xTi_2O_5$ at $x = 0.03$ were 748 and 742 K, respectively. The electrical conductivity ($\sigma$) of single-crystalline $Ba_{1-x}Sr_xTi_2O_5$ was higher than that of poly-crystalline $Ba_{1-x}Sr_xTi_2O_5$. Larger size of single-crystalline $Ba_{1-x}Sr_xTi_2O_5$ specimen than that of $BaTi_2O_5$ was obtained.
[doi:10.2320/matertrans.48.984]

(Received November 1, 2006; Accepted February 23, 2007; Published April 25, 2007)

***Keywords:*** *$Ba_{1-x}Sr_xTi_2O_5$, arc-melting, poly-crystal, floating-zone (FZ) melting, single-crystal, ac impedance spectroscopy*

## 1. Introduction

Barium titanate ($BaTiO_3$, BT) is a well-known lead-free ferroelectric material with a sharp peak of permittivity at the Curie temperature ($T_c$) about 400 K.[1)] Many attentions have been paid on the effect of substitution for BT to modify the $T_c$ and to flatten the peak of permittivity.[2–5)] In particular, $Ba_{1-x}Sr_xTiO_3$ (BST) has been much interested because of the wide-ranged substitution of SrO in BT.[6–8)] Although both poly- and single-polycrystalline BST exhibited the decrease in $T_c$ and the increase in peak permittivity with increasing SrO substitution, single-crystalline BST showed more significant effect of substitution on dielectric property than poly-crystalline BST.[9–14)]

We and Akishige *et al.* independently reported that $BaTi_2O_5$ ($BT_2$) is a ferroelectric compound of a high Curie temperature ($T_c = 750$ K), and the space group of $BT_2$ was determined as monoclinic *C*2 consisting with the ferroelectricity in the b-direction.[15–20)] However, the $BT_2$ single crystal with a large size can be hardly prepared because of the cleavage parallel to the growth direction. $BT_2$ may decompose to BT and $Ba_6Ti_{17}O_{40}$ ($B_6T_{17}$) in a temperature range between 1423 and 1585 K.[16,21)] This may cause the difficulty of obtaining large-size single-crystalline $BT_2$. We have prepared *b*-axis orientated $Ba_{1-x}Sr_xTi_2O_5$ ($x = 0.03$ to 0.1) by arc-melting and reported that a small amout of SrO substitution can significantly improve the dielectric property of $Ba_{1-x}Sr_xTi_2O_5$. In the present study, we have prepared *b*-axis oriented poly- and a large size single-crystalline $Ba_{1-x}Sr_xTi_2O_5$ with SrO substitution of $x < 0.03$ by arc- and FZ (Floating Zone) melting, respectively, and studied the effect of SrO substitution on the dielectric property of poly- and single-crystalline $Ba_{1-x}Sr_xTi_2O_5$.

## 2. Experimental Procedures

$TiO_2$, $BaCO_3$, and $SrCO_3$ (99.9% purity) powders were mixed in a molar ratio of $(Ba + Sr)/Ti = 1/2$, and the molar fraction of $SrCO_3$ was changed from 0 to 0.03. The mixed powders were pressed into pellets with 20 mm in diameter at 10 MPa, and calcined at 1223 K for 43 ks in air. The pellets were arc-melted on a water-cooled copper plate in an Ar atmosphere. The mixed powders were also isostatically pressed in a latex tube with 10 mm in diameter, and sintered at 1503 K for 43 ks in air. The sintered rods were melted and directionally solidified by an FZ method at a rate of $5.6 \times 10^{-6}$ ms$^{-1}$ in a flowing Ar-$O_2$ gas. The crystal orientation was identified by X-ray diffraction (CuK$\alpha$). The specimens were cut perpendicularly to (010) plane and the dielectric properties were measured using an AC impedance analyzer (Hewlett Parckard 4194A) at frequencies (f) from $10^2$ to $10^7$ Hz and at temperatures from 293 to 1073 K in air. Composition of specimens was analyzed by an electron probe microanalysis (EPMA).

## 3. Results and Discussion

Figure 1 shows the appearance of specimens prepared by FZ. The single-crystalline $Ba_{1-x}Sr_xTi_2O_5$ had a cleavage plane of (001), same as that of $BT_2$. Single-crystalline $Ba_{0.99}Sr_{0.01}Ti_2O_5$ 4 mm in diameter and 16 mm in length was cut. This size was larger than that of single-crystalline $BT_2$ without SrO substitution.[15,19)] Kojima *et al.* reported that a

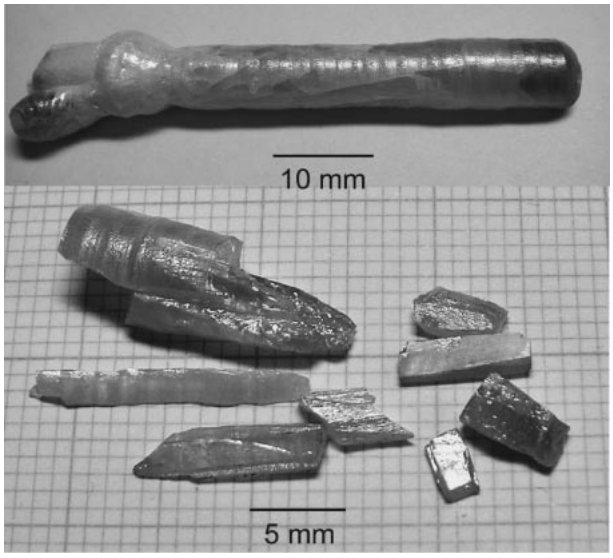


Fig. 1 Specimens obtained by FZ melting.

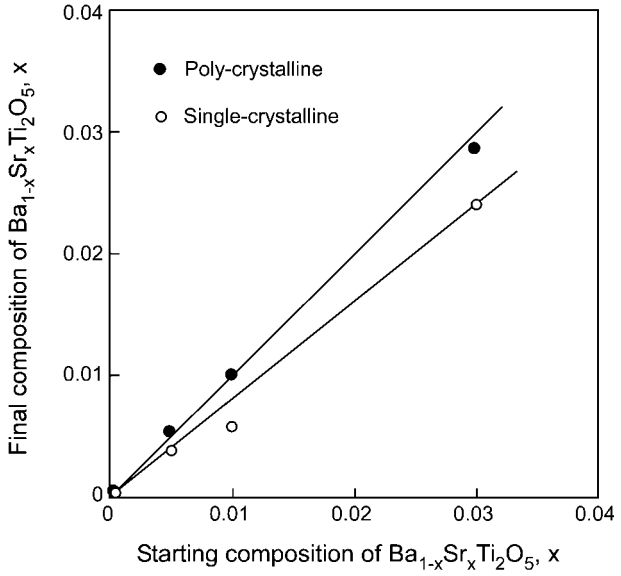


Fig. 2 Relationship between the starting composition of $Ba_{1-x}Sr_xTi_2O_5$ sintered bodies and the final composition of poly- and single-crystalline $Ba_{1-x}Sr_xTi_2O_5$ prepared by arc-melting and FZ-melting.

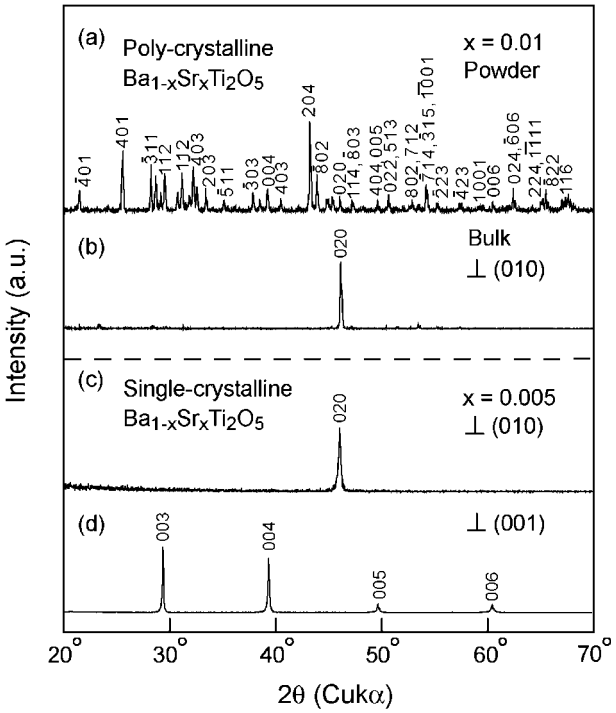


Fig. 3 XRD patterns of poly- and single-crystalline $Ba_{1-x}Sr_xTi_2O_5$.

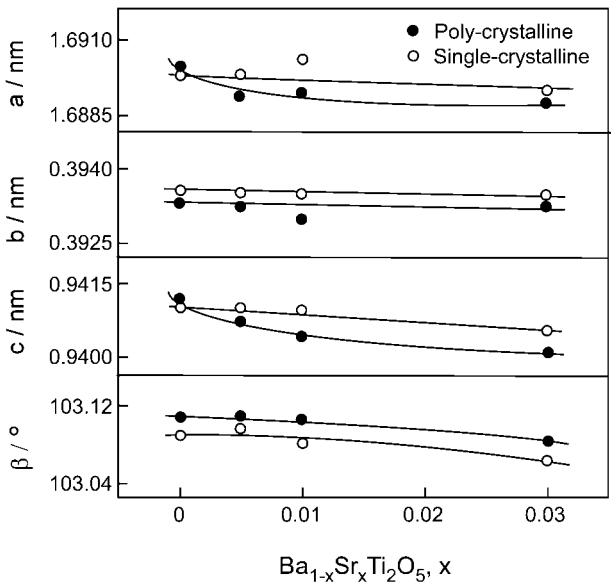


Fig. 4 Effect of SrO concentration on lattice parameters of poly- and single-crystalline $Ba_{1-x}Sr_xTi_2O_5$.

small amount of SrO substitution was effective to prepare large-size single-crystalline BT.[14,22] The SrO substitution in $BT_2$ might enable one to obtain large-size single-crystalline $Ba_{1-x}Sr_xTi_2O_5$. The SrO distribution in the as-grown crystals prepared by FZ melting was almost uniform (±0.02%) except the initial and final growth regions. Figure 2 demonstrates the relationship between the nominal starting composition of $Ba_{1-x}Sr_xTi_2O_5$ sintered bodies and the final composition of poly- and single-crystalline $Ba_{1-x}Sr_xTi_2O_5$ prepared by arc-melting and FZ-melting, respectively. The Sr concentration in the as-grown crystals was slightly lower than that in the $Ba_{1-x}Sr_xTi_2O_5$ sintered bodies. The fast cooling speed in present FZ method would cause a non-equilibrium solidification. Nevertheless the solidification has reached to a steady state with the effective distribution coefficient being less than unity. The detail of the distribution coefficients can be available in literatures.[23] Kojima *et al.* reported that the Sr concentration in as-grown BST crystals almost agreed with those of starting composition at $x < 0.05$ in an FZ method.[14] Since $BaTiO_3$ is a simple perovskite, $Ba^{2+}$ ions could be easily substituted by $Sr^{2+}$ ions. However, $BT_2$ has a monoclinic crystal structure with complicated corner and edge shared $TiO_6$ octahedra, and therefore $Sr^{2+}$ substitution in $BT_2$ might be more difficult than that in BT. In the following, the compositions of $Ba_{1-x}Sr_xTi_2O_5$ in both poly- and single-crystalline specimens were represented as the nominal starting composition of $Ba_{1-x}Sr_xTi_2O_5$ sintered bodies.

Figure 3 shows the XRD patterns of poly- and single-crystalline $Ba_{1-x}Sr_xTi_2O_5$. The powder XRD pattern showed that poly-crystalline $Ba_{0.99}Sr_{0.01}Ti_2O_5$ was in a single phase of $BT_2$ (Fig. 3(a)). We have already reported that the solubility limit of SrO in $BT_2$ would be about 10 mol%. The XRD pattern of poly-crystalline $Ba_{1-x}Sr_xTi_2O_5$ plate showed a significant (020) orientation (Fig. 3(b)). Columnar grains perpendicular to the water-cooled copper plate were observed in the cross section of specimens by SEM. The XRD pattern of single-crystalline $Ba_{0.995}Sr_{0.005}Ti_2O_5$ plate perpendicular and parallel to the growth direction showed only the (020) and (001) peaks, corresponding to a strong *b*-axis orientation as depicted in Fig. 3(c) and (d), respectively.

Figure 4 demonstrates the effect of SrO content on the lattice parameter of poly- and single-crystalline $Ba_{1-x}Sr_x$-$Ti_2O_5$. The lattice parameter decreased with increasing $x$ for both poly- and single-crystalline $Ba_{1-x}Sr_xTi_2O_5$. However, the decrease in lattice parameter of the poly-crystalline specimens was slightly more significant than that of single-crystalline specimens. This may be caused of the higher Sr content in the poly-crystalline specimens as shown in Fig. 2;

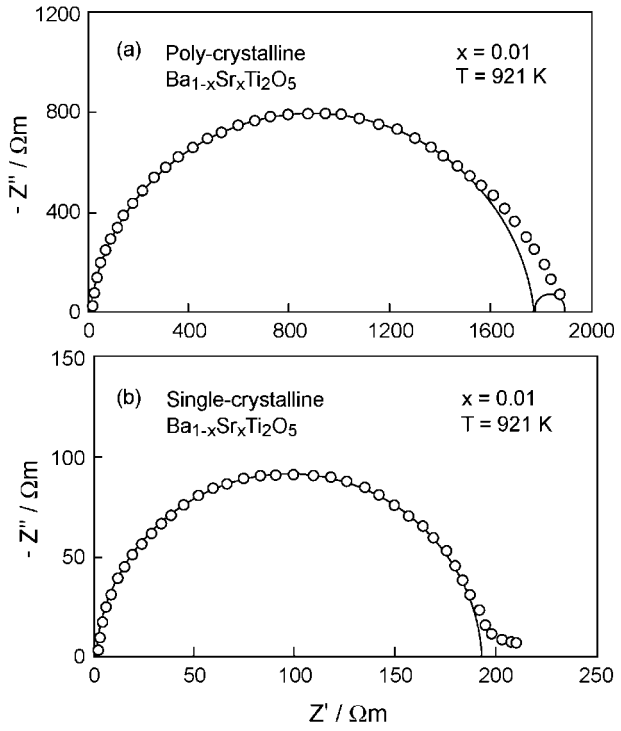


Fig. 5 Cole-Cole plots of $Ba_{1-x}Sr_xTi_2O_5$: poly-crystalline (a) and single-crystalline (b).

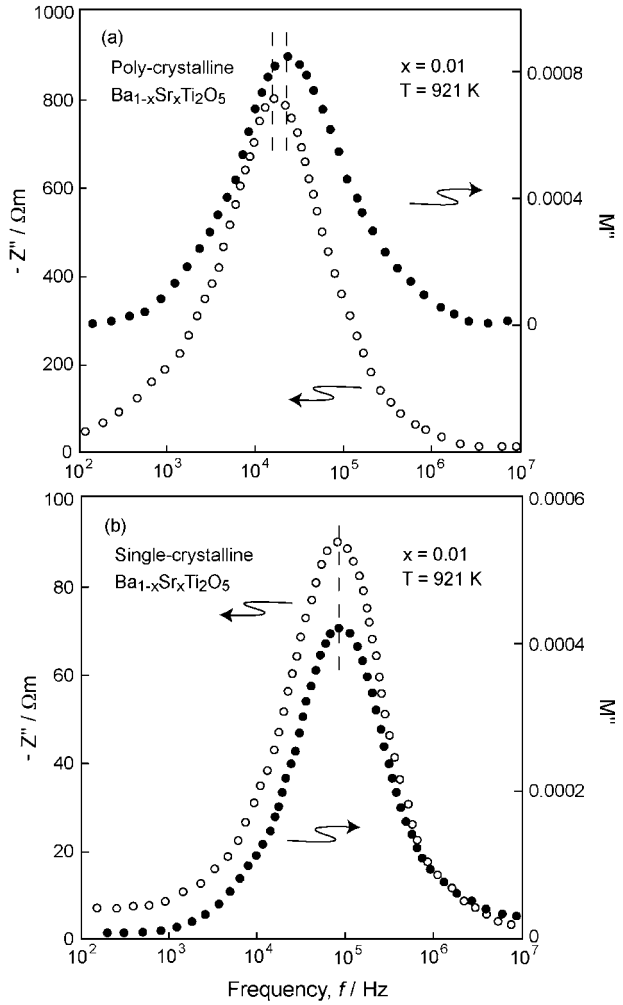


Fig. 6 M″ and Z″ of $Ba_{1-x}Sr_xTi_2O_5$ as a function of frequency: poly-crystalline (a) and single-crystalline (b).

the higher Sr concentration in $Ba_{1-x}Sr_xTi_2O_5$, the lower lattice parameters.

Figure 5 shows the Cole-Cole plots of poly- and single-crystalline $Ba_{1-x}Sr_xTi_2O_5$. An equivalent electrical circuit with series combination of parallel R (resistance) and C (capacitance) elements can be employed to analyse the electrical characteristics of material. The number and shape of semicircles in the Cole-Cole plot would indicate components in the material. In the Cole-Cole plot of poly-crystalline $Ba_{0.99}Sr_{0.01}Ti_2O_5$, one depressed semicircle was observed. That may be deconvoluted into two semicircles implying a bulk and additional component. Although a second phase was not clearly detected in the poly-crystalline $Ba_{0.99}Sr_{0.01}Ti_2O_5$ by XRD, a small amount of BT and $Ba_6Ti_{17}O_{40}$ ($B_6T_{17}$) due to the partial decomposition of $BT_2$ was identified by electron probe microanalysis (EPMA). The main circle in a higher frequency range and the small circle in a lower frequency range might be contributed by the $BT_2$ bulk and the second phases due to associate capacitance values of $1.31 \times 10^{-10}$ F and $5.7 \times 10^{-8}$ F,[24,25] respectively (Fig. 5(a)). The Cole-Cole plot of single-crystalline $Ba_{0.99}Sr_{0.01}Ti_2O_5$ may be contributed by only single semicircle by the $BT_2$ bulk response due to the small capacitance value of $2.4 \times 10^{-10}$ F (Fig. 5(b)).

Figure 6 depicts the imaginary parts of complex impedance (Z″) and modulus (M″) of poly- and single-crystalline $Ba_{1-x}Sr_xTi_2O_5$ as a function of frequency (f) at 921 K. The plots of Z″ and M″ vs. f of the poly-crystalline $Ba_{0.99}Sr_{0.01}Ti_2O_5$ showed a difference of peak frequencies. These peak frequencies were almost in agreement with the frequency of the top of the first semicircle shown in Fig. 5(a) consisting with the bulk response. Since the peak frequency of the Z″ vs. f and M″ vs. f plots can be calculated from the equation of $2\pi fRC = 1$, they should have been coincided in theory. The discrepancy of these peak frequencies has been often reported.[26,27] Some defect structure by the rapid quenching or the second phase by the partial decomposition may cause the discrepancy of the peak frequencies. On the other hand, the single crystalline $Ba_{0.99}Sr_{0.01}Ti_2O_5$ had the same peak frequency in the Z″ and M″ vs. f plots as shown in Fig. 6(b), due to minimal defect or second phase in the single-crystalline specimen.

Figure 7 shows the temperature dependence of permittivity of poly- and single-crystalline $Ba_{1-x}Sr_xTi_2O_5$. The peak permittivity at the $T_c$ changed depending on $x$. The permittivity of poly-crystalline $Ba_{1-x}Sr_xTi_2O_5$ showed the maximum permittivity at $x = 0.01$ (Fig. 7(a)). The permittivity of the single-crystalline $Ba_{1-x}Sr_xTi_2O_5$ showed the much sharper and higher peaks than poly-crystalline specimens at the $T_c$. The lower permittivity of poly-crystalline specimens may be caused of the imperfectness of $b$-axis orientation and crystal defects (Fig. 7(b)). Since the poly-crystalline $Ba_{1-x}Sr_xTi_2O_5$ was prepared by arc-melting in an Ar atmosphere, as-grown specimens were black in color suggesting oxide vacancies. Although the poly-crystalline specimens were heat-treated in air at 1323 K for 43 ks to compensate oxide vacancies, some defects could be remained

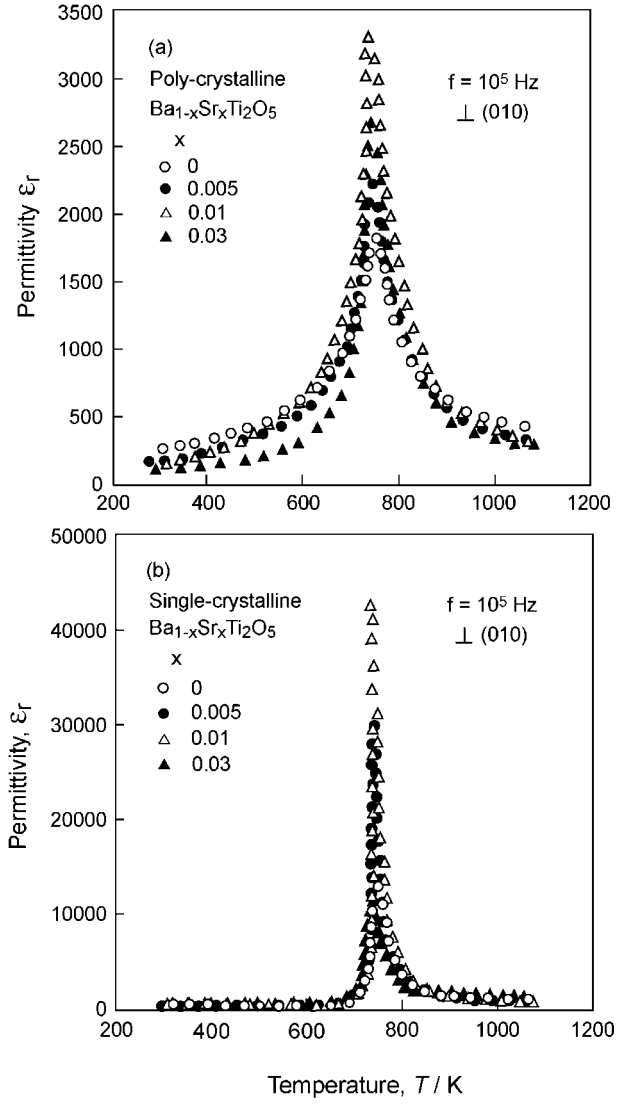


Fig. 7 Temperature dependence of permittivity of $Ba_{1-x}Sr_xTi_2O_5$ at $f = 10^5$ Hz: poly-crystalline (a) and single-crystalline (b).

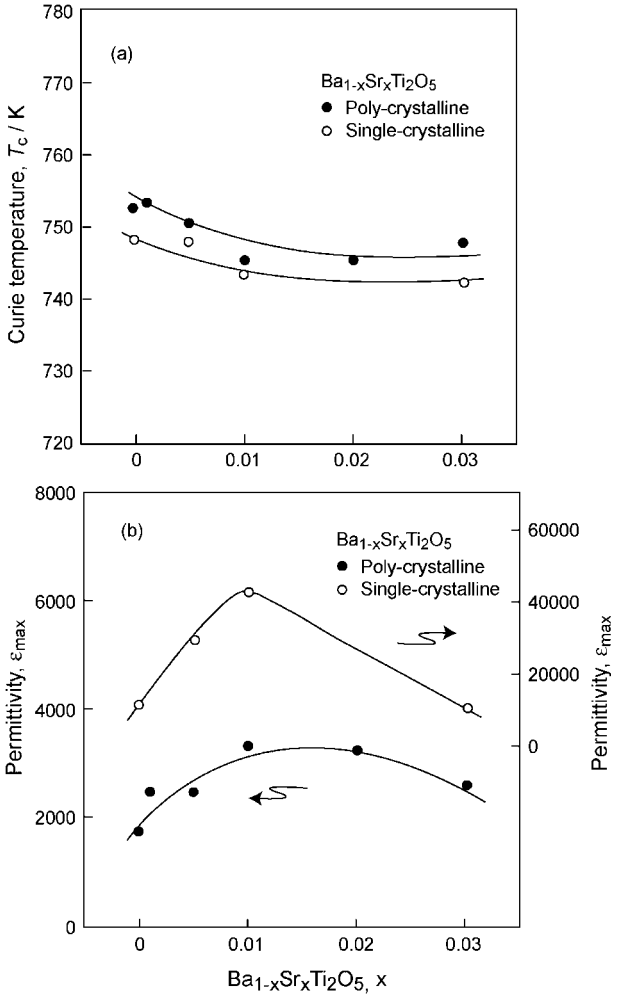


Fig. 8 Effect of SrO content on $\varepsilon_{max}$ and $T_c$ for $Ba_{1-x}Sr_xTi_2O_5$ at $f = 10^5$ Hz: $\varepsilon_{max} - x$ plot (a) and $T_c - x$ plot (b).

in the specimens. Akishige *et al.* reported that the single-crystalline $BT_2$ grown in a reducing atmosphere showed a broad peak around $T_c$, implying that the oxide vacancies would associate with the dielectric dispersion.[18] The difference of lattice parameter between poly- and single-crystalline $Ba_{1-x}Sr_xTi_2O_5$ could suggest the local segregation of $Sr^{2+}$. This might also cause the decrease in the permittivity of poly-crystalline $Ba_{1-x}Sr_xTi_2O_5$.

Figure 8 demonstrates the effect of $x$ on the $T_c$ and the peak permittivity ($\varepsilon_{max}$) of poly- and single-crystalline $Ba_{1-x}Sr_xTi_2O_5$ at the $T_c$. The $T_c$ of poly-crystalline $Ba_{1-x}Sr_xTi_2O_5$ decreased from 752 to 748 K with increasing $x$ from 0 to 0.03. The $T_c$ of single-crystalline $Ba_{1-x}Sr_xTi_2O_5$ decreased from 748 to 742 K with increasing $x$ from 0 to 0.03 (Fig. 8(a)). The $T_c$ of BST decreased linearly from 405 to 392 K with increasing $x$ from 0 to 0.03, implying more sensitive to the $Sr^{2+}$ substitution compared to that of $Ba_{1-x}Sr_xTi_2O_5$.[28,29] The solubility limit of $Sr^{2+}$ in $BT_2$ was much lower than that in BT because of the more complicated crystal structure of $BT_2$. The smaller solubility of $Sr^{2+}$ in $BT_2$ may result in the smaller change of $T_c$ than that in BT. The maximum permittivity of poly- and single crystalline $Ba_{1-x}Sr_xTi_2O_5$ were 3300 and 42190 at $x = 0.01$, respectively (Fig. 8(b)).

Figure 9 shows the temperature dependence of reciprocal permittivity ($\varepsilon^{-1}$) of poly- and single-crystalline $Ba_{1-x}Sr_xTi_2O_5$. The $\varepsilon^{-1}$ of both specimens obeyed the Curie-Weiss law at temperatures higher than the $T_c$. The Curie-Weiss temperature ($T_0$) of poly-crystalline $Ba_{0.99}Sr_{0.01}Ti_2O_5$, 718 K, was lower than the $T_c$, while that of single-crystalline $Ba_{0.99}Sr_{0.01}Ti_2O_5$ was almost in agreement with the $T_c$. In the case of BST, the difference between $T_0$ and $T_c$ was 5 to 10 K for single-crystalline[30] whereas 15 to 30 K for polycrystalline specimens.[31] It is commonly understood that the $T_0$ is always lower than $T_c$, which suggests the first order transformation. In the present study, the difference between $T_c$ and $T_0$ of $Ba_{1-x}Sr_xTi_2O_5$ specimens was almost the same as that of BT, about 5 and 25 K for single-crystalline and poly-crystalline specimens, respectively. The phase transformation mechanism of $BT_2$ has been studied by Yashima *et al.*, and reported that $BT_2$ would transform from $C2$ to $C2/m$ likely to be the first order transformation.[32]

Figure 10 shows the temperature dependence of electrical conductivities ($\sigma$) of poly- and single-crystalline $Ba_{1-x}Sr_xTi_2O_5$. The $\sigma$ of both specimens increased with the increasing

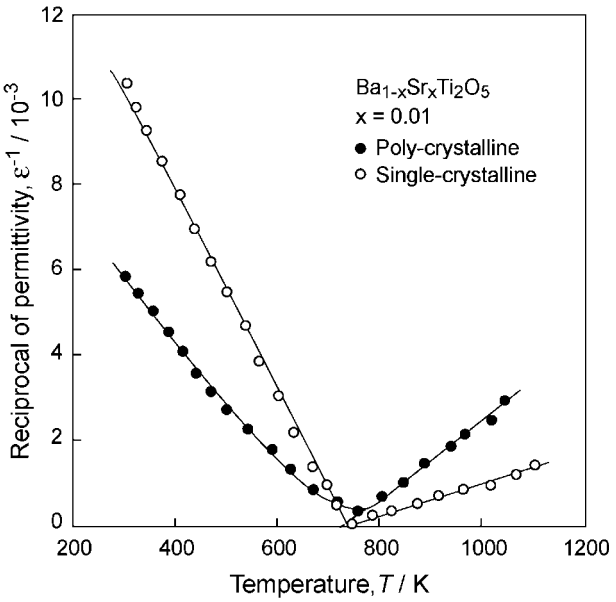


Fig. 9 Temperature dependence of $\varepsilon^{-1}$ of poly- and single-crystalline $Ba_{1-x}Sr_xTi_2O_5$ perpendicular to (010) plane at $f = 10^5$ Hz.

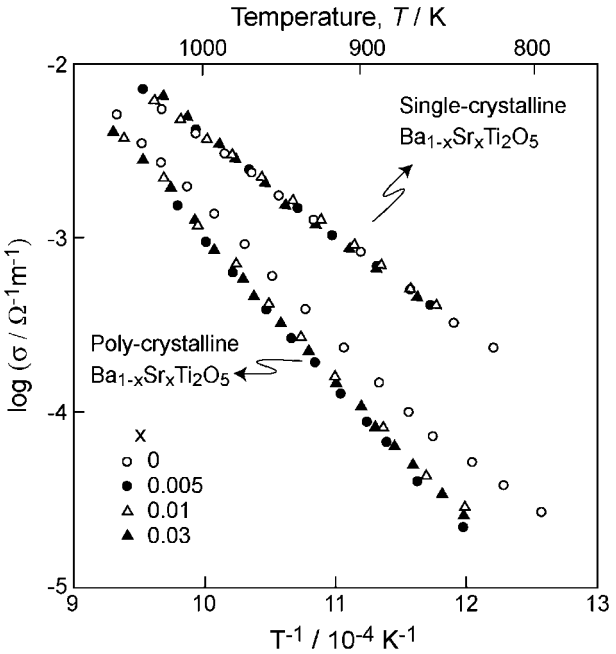


Fig. 10 Temperature dependence of $\sigma$ of poly- and single-crystalline $Ba_{1-x}Sr_xTi_2O_5$.

temperature. The $\sigma$ of single-crystalline $Ba_{1-x}Sr_xTi_2O_5$ was higher than that of poly-crystalline $Ba_{1-x}Sr_xTi_2O_5$. The $\sigma$ of poly-crystalline $Ba_{1-x}Sr_xTi_2O_5$ was lower than that of poly-crystalline $BT_2$, while the $\sigma$ of single-crystalline $Ba_{1-x}Sr_xTi_2O_5$ was almost same with single-crystalline $BT_2$. For single-crystalline $BT_2$, the $\sigma$ in the b direction was higher than those in the a and c directions.[33] The $\sigma$ of poly-crystalline $Ba_{1-x}Sr_xTi_2O_5$ was lower than that of single-crystalline specimens. This may be caused of the imperfectness of b-direction orientation and the scattering at grain boundary and local segregation. The activation energy ($E_a$) of

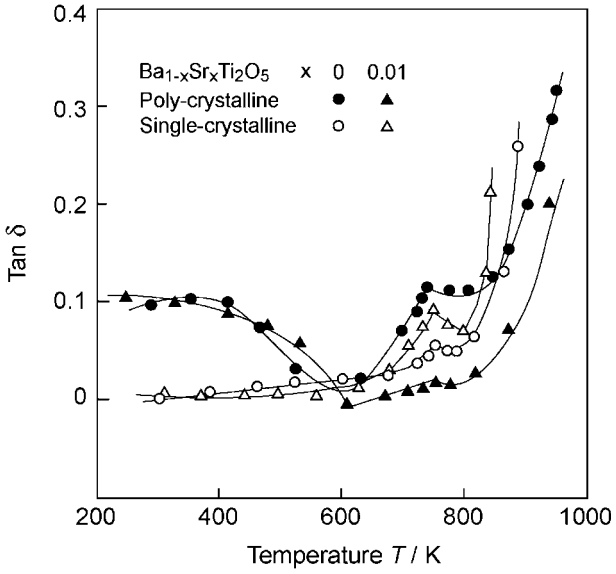


Fig. 11 Temperature dependence of tan $\delta$ of poly- and single-crystalline $Ba_{1-x}Sr_xTi_2O_5$.

poly-crystalline $Ba_{1-x}Sr_xTi_2O_5$ was about 1.62 eV, while the $E_a$ of single-crystalline $Ba_{1-x}Sr_xTi_2O_5$ was about 1.01 eV. These values were independent of SrO content.

Figure 11 depicts the temperature dependence of dielectric loss (tan $\delta$) of poly- and single-crystalline $Ba_{1-x}Sr_xTi_2O_5$ at $f = 10^5$ Hz. At lower temperature range ($T < 400$ K) the tan $\delta$ of poly-crystalline $Ba_{1-x}Sr_xTi_2O_5$ was higher than that of single-crystalline $Ba_{1-x}Sr_xTi_2O_5$. At the higher temperature range ($T > T_c$) both of them showed a sharp increase because of the increase in electric conduction. The peaks of tan $\delta$ near the $T_c$ could be caused by the general Kramers-Kronig relationship; the higher $\varepsilon'$, the higher $\varepsilon''$.

## 4. Conclusions

Strongly *b*-axis oriented poly- and single-crystalline $Ba_{1-x}Sr_xTi_2O_5$ were prepared by arc-melting and FZ, respectively. A single-crystalline $Ba_{0.99}Sr_{0.01}Ti_2O_5$ of 4 mm in diameter and 16 mm in length was obtained. The permittivity of poly- and single-crystalline $Ba_{1-x}Sr_xTi_2O_5$ showed the maximum at $x = 0.01$. The highest permittivities of poly- and single-crystalline $Ba_{1-x}Sr_xTi_2O_5$ were of 3300 and 42190, respectively. The $T_c$ of poly- and single-crystalline $Ba_{1-x}Sr_xTi_2O_5$ decreased from 752 to 748 K and from 748 to 742 K, respectively, with increasing $x$ from 0 to 0.03. The $\sigma$ of single-crystalline $Ba_{1-x}Sr_xTi_2O_5$ was higher than that of poly-crystalline $Ba_{1-x}Sr_xTi_2O_5$. The tan $\delta$ of single-crystalline $Ba_{1-x}Sr_xTi_2O_5$ was smaller than that of poly-crystalline specimen.

## Acknowledgements

The study was financially supported by the Grant-in-Aids for Exploratory Research (17656209) of the Ministry of Education Culture Sports, Science and Technology (MEXT) and by the JSPS-KOSEF Asian CORE University Program of the Japan Society for the Promotion of Science (JSPS).

## REFERENCES


1) F. D. Morrison, D. C. Sinclair and A. R. West: J. Appl. Phys. **86** (1999) 6355–6366.
2) A. D. Hilton and B. W. Ricketts: J. Phys. D: Appl. Phys. **29** (1996) 1321–1325.
3) D. Hennings and A. Schnell: J. Am. Ceram. Soc. **65** (1982) 539–544.
4) N. Maso, H. Beltran, E. Cordoncillo, A. A. Flores, P. Escribano, D. C. Sinclair and A. R. West: J. Mater. Chem. **16** (2006) 3114–3119.
5) N. Maso, H. Beltran, E. Cordoncillo, P. Escribano and A. R. West: J. Mater. Chem. **16** (2006) 1626–1633.
6) H. Abdelkefi, H. Khemakhem, G. Velu, J. C. Carru and R. V. Muhll: J. Alloys and Compounds **399** (2005) 1–6.
7) B. Su, J. E. Holmes, B. L. Cheng and T. W. Button: J. Electroceramics. **9** (2002) 111–116.
8) L. Szymczak, Z. Ujma, J. Handerek and J. Kapusta: Ceramics International **30** (2004) 1003–1008.
9) X. Wei and X. Yao: Mater. Sci. Eng. **B99** (2003) 74–78.
10) L. Zhou, P. M. Vilarinho and J. L. Baptista: J. Euro. Cera. Soci. **19** (1999) 2015–2020.
11) M. Valant and D. Suvorov: J. Am. Ceram. Soc. **87** (2004) 1222–1226.
12) F. Brown and W. H. Todtf: J. Appl. Phys. **35** (1964) 1594–1598.
13) K. Bethe and F. Welz: Mat. Res. Bull. **6** (1971) 209–218.
14) H. Kojima, M. Watanabe and I. Tanaka: J. Crystal Growth **155** (1995) 70–74.
15) T. Kimura, T. Goto, H. Yamane, H. Iwata, T. Kajiwara and T. Akashi: Acta. Cryst. **C59** (2003) i128–i130.
16) T. Akashi, H. Iwata and T. Goto: Mater. Trans. **44** (2003) 802–804.
17) T. Akashi, H. Iwata and T. Goto: Mater. Trans. **44** (2003) 1644–1646.
18) Y. Akishige, K. Fukano and H. Shigematsu: J. Electroceramics. **13** (2004) 561–565.
19) Y. Akishige: Jpn. J. Appl. Phys. **44** (2005) 7144–7147.
20) Y. Akishige, K. Fukano and H. Shigematsu: Jpn. J. Appl. Phys. **42** (2003) L946–L948.
21) G. Pfaff: J. Mater. Sci. Lett. **9** (1990) 1145–1147.
22) J. Furukawa and T. Tsukamoto: Jpn. J. Appl. Phys. **30** (1991) 2391–2393.
23) W. G. Pfann: *Zone Melting*, (John Wiley & Sons, Inc.) 7–22.
24) J. T. S. Irvine, D. C. Sinclair and A. R. West: Advanced Materials **2** (1990) 132–138.
25) T. J. Hwang and G. M. Choi: Sensors and Actuators **B40** (1997) 187–191.
26) R. Gerhardt: J. Phys. Chem. Solids. **55** (1994) 1491–1506.
27) M. A. L. Nobre and S. Lanfredi: J. Appl. Phys. **93** (2003) 5576–5582.
28) D. Rytz, B. A. Wechsler, K. W. Kirby and C. C. Nelson: Jpn. J. Appl. Phys., Suppl. **24-2** (1985) 622–624.
29) B. A. Wechsler and K. W. Kirby: J. Am. Ceram. Soc. **75** (1992) 981–984.
30) M. E. Drougard and D. R. Young: Phys. Rev. **95** (1954) 1152–1153.
31) H. Abdelkefi, H. Khemakhem, G. Velu, J. C. Carru and R. Von der Muhll: J. Alloys Compounds **399** (2005) 1–6.
32) M. Yashima, R. Tu, Takashi Goto and H. Yamane: Appl. Phys. Lett. **87** (2005) 101909-1-101909-3.
33) R. Tu and T. Goto: Mater. Trans. **47** (2006) 2898–2903.